ISSN 1330–0016
CODEN FIZBE7

INVESTIGATION OF EXOTIC ${}^{6}_{\Lambda\Lambda}$He HYPERNUCLEI BY THE HYPERSPHERICAL THREE-BODY METHOD

MD. A. KHAN and T. K. DAS

Department of Physics, University of Calcutta, 92, Acharya Prafulla Chandra Road, Calcutta - 700009, India.

Received 17 April 1999; revised manuscript received 8 November 1999
Accepted 6 July 2000

We critically review the $\Lambda\Lambda$ dynamics by examining several $\Lambda\Lambda$ and $\Lambda\alpha$ phenomenological potentials in the study of the bound state properties of ${}^{6}_{\Lambda\Lambda}$He, as a three-body system. The hyperspherical harmonics expansion method, which is an essentially exact method, has been employed for the three-body system. A convergence in binding energy up to 0.07% for $K_{\max} = 20$ has been achieved. In our calculation, we made no approximation in restricting the allowed l-values of the interacting pair.

PACS numbers: 21.80.+a, 21.60.Jz, 21.30.Fe UDC 535.217, 539.21

Keywords: Raynal Revai coefficient, hyperspherical harmonics expansion, ${}^{6}_{\Lambda\Lambda}$He multistrange hypernucleus

1. Introduction

The study of the structure of light exotic hypernuclei have become an area of particular interest since the discovery of this species in the early sixties. Important members of this new species are the nuclei ${}^{6}_{\Lambda\Lambda}$He, ${}^{10}_{\Lambda\Lambda}$Be and ${}^{13}_{\Lambda\Lambda}$B [1–4]. Discovery of these doubly Λ-hypernuclei opened a new avenue to extract important informations about the $\Lambda\Lambda$ interaction. This enhances the range of ones imagination on the possible existence of multistrange hypernuclei. In the early stages, the emulsion experiments provided a source of information on hypernuclei, which was limitted to binding energies of Λ-particle in the light hypernuclei and the decay rates (lifetimes) [2]. The binding energy data provided physicists some qualitative informations about the Λ-nucleon (ΛN) interaction and single particle potential strength for Λ-particle in hypernuclei [5]. The hyperon – nucleon scattering experiments have also been performed, but these are still in the primary stages and do not provide detailed phase shifts to construct reliably the potential. Some ΛN and ΣN total cross-sections and very few angular distributions at low energies have been measured [6–11], but are not sufficient to allow the phase shift analysis. Nevertheless, the bound state properties of single and double Λ-hypernucleus can give valuable indirect information about ΛN and ΛΛ interactions. One can for example take phenomenological forms of ΛN and ΛΛ interactions and see if they reproduce the observables of the hypernuclei. Alternatively, one can adjust the parameters of the empirical potential to reproduce the bound state properties and thus predict the effective ΛN and ΛΛ interactions. Earlier attempts in this direction [12–15] used variational and approximate few-body calculations, treating the hypernucleus as a few-body system. In the present work, we review the $\alpha\Lambda$ and ΛΛ interactions by studying the general properties of ${}^{6}_{\Lambda\Lambda}$He treated as a three-body system. The ${}^{6}_{\Lambda\Lambda}$He hypernucleus consisting of two protons, two neutrons and two Λ-hyperons is considered to have a $(0s)^6$ type configuration. Thus, it may constitute the lightest closed shell of the p, n, Λ system with a complete analogy to ^{4}He in the p, n system. Here we consider the internal structure, stability and compactness of the ${}^{6}_{\Lambda\Lambda}$He nucleus. The observed separation energy of a Λ-particle in ${}^{6}_{\Lambda\Lambda}$He is 7.6 MeV [16], which is evidently smaller than that of a nucleon (≈ 20 MeV) in ^{4}He. Certainly the ${}^{6}_{\Lambda\Lambda}$He nucleus falls behind the α-particle in energetic stabilty. No ΛΛ bound state has been reported.

We employ the hyperspherical harmonics expansion (HHE) method to solve such a three-body system. This method is a powerful tool for the *ab initio* solution of the few-body Schrödinger equation for a given set of interaction potentials among the constituent particles. This method has been used for bound states in atomic [17–34], nuclear [35–52] and particle physics [53–55]. Attempts have been made to use it in scattering problems as well [56]. In this method, the wave function is expanded in a complete set of hyperspherical harmonics (HH), which, for a three-body system, are the six-dimensional analog of the angular part of eigenfunctions of the 3-dimensional Laplacian operator. The resulting Schrödinger equation is a set of coupled differential equations which can be solved numerically by the renormalized Numerov method (RNM) [57–58] or the hyperspherical adiabatic approximation (HHA) [61]. The HHE method is essentially an exact one and more reliable than other methods. It involves no approximation except for an possible truncation of the expansion basis. By gradually expanding the expansion basis and checking the rate of convergence, any desired precision in the binding energy can, in principle, be achieved. However, the number of coupled differential equations and, therefore, the complexity in the numerical solution increases rapidly as the expansion basis is increased by including larger hyper-angular-momentum quantum number. Computer limitations set an ultimate limit to the attainable precision. Thus, in this approach, the attainment of desired convergence in physical observables are of great importance.

In the present calculation, we achieved a convergence of the binding energy to within 0.07%. In addition to the two-Λ separation energy which is defined as

$$B_{\Lambda\Lambda}({}^{A}_{\Lambda\Lambda}Z) = M({}^{A-2}Z) + 2M_{\Lambda} - M({}^{A}_{\Lambda\Lambda}Z), \tag{1}$$

we have also studied the size, density distribution and correlation among the ^{4}He (core) and the valence Λ-hyperons.

This paper is organized as follows: In Sect. 2, we review the HHE method for a three-body system consisting of non-identical particles. Results of the calculation and discussion are presented in Sect. 3. Finally, in Sect. 4 we draw our conclusions.

2. *Hyperspherical harmonics expansion method*

We label the ^{4}He-core as particle '1' and the two valence Λ-particles as particles '2' and '3' (see Fig. 1.). For pairwise interactions, we can treat any one of the three particles as the spectator, remaining two being the interacting pair. Thus, there are three possible partitions labelled 'i' (i=1, 2, 3). In

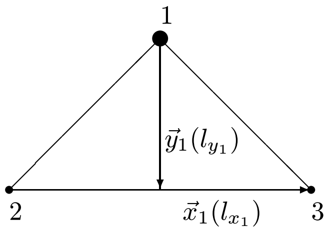

Fig. 1. Choice of Jacobi coordinates for the partition '1'.

the partition 'i', particle numbered 'i' is the spectator and particles numbered 'j' and 'k' form the interacting pair ($i, j, k = 1, 2, 3$, cyclic). For a given partition 'i', the Jacobi coordinates (which are proportional to the relative separation between the particles of the interacting pair and the relative separation between the spectator and the centre of mass of the interacting pair respectively) are defined as

$$\begin{aligned} \vec{x}_i &= \left[\frac{m_j m_k M}{m_i (m_j + m_k)^2}\right]^{\frac{1}{4}} (\vec{r}_j - \vec{r}_k) \\ \vec{y}_i &= \left[\frac{m_i (m_j + m_k)^2}{m_j m_k M}\right]^{\frac{1}{4}} \left(\vec{r}_i - \frac{m_j \vec{r}_j + m_k \vec{r}_k}{m_j + m_k}\right) \\ \vec{R} &= \frac{1}{M} (m_i \vec{r}_i + m_j \vec{r}_j + m_k \vec{r}_k) \end{aligned} \tag{2}$$

(i, j, k=1, 2, 3 cyclic) where m_i, $\vec{r}_i$ are the mass and position of the i^{th} particle and $M = m_i + m_j + m_k$ is the total mass and $\vec{R}$ is the centre of mass of the system. The sign of $\vec{x}_i$ is fixed by the condition that 'i', 'j', 'k' form a cyclic permutation of (1, 2, 3). In the transformation (2), the six dimensional volume element is conserved (i.e. the Jacobian is unity) and the centre-of-mass motion is automatically separated. The relative motion of the three-body system is described by the Schrödinger equation

$$\left[-\frac{\hbar^2}{2\mu}(\nabla^2_{x_i} + \nabla^2_{y_i}) + V_{jk}(\vec{x}_i) + V_{ki}(\vec{x}_i, \vec{y}_i) + V_{ij}(\vec{x}_i, \vec{y}_i) - E\right] \Psi(\vec{x}_i, \vec{y}_i) = 0 \tag{3}$$

where $\mu = (m_i m_j m_k/M)^{1/2}$ is an effective mass parameter and V_{ij} is the interaction potential between $i^{\rm th}$ and $j^{\rm th}$ particles. We next introduce the hyperspherical variables defined by [52]

$$\begin{aligned} x_i &= \rho\cos\phi_i\,, \\ y_i &= \rho\sin\phi_i\,, \end{aligned} \qquad (4)$$

where $\rho = \sqrt{x_i^2 + y_i^2}$ is the global length (also called the hyper-radius), which is invariant under three-dimensional rotations and permutations of the particle indices. Thus, ρ is the same for all three partitions. The five other hyperspherical variables include the hyperspherical angle $\phi_i = \tan^{-1}(y_i/x_i)$ and the polar angles $(\theta_{x_i}, \phi_{x_i})$ and (θ_{y_i}, ϕ_{y_i}) giving orientations of $\vec{x}_i$ and $\vec{y}_i$, respectively. These are collectively denoted by

$$\Omega_i \equiv \{\phi_i, \theta_{x_i}, \phi_{x_i}, \theta_{y_i}, \phi_{y_i}\} \qquad (5)$$

and are called the "hyperangles". The six-dimensional volume element is given by

$$dV_6 = \rho^5\ \mathrm{d}\rho\ \cos^2\phi_i\ \sin^2\phi_i\ \mathrm{d}\phi_i\ \mathrm{d}\Omega_{x_i}\ \mathrm{d}\Omega_{y_i}\,, \qquad (6)$$

where

$$\begin{aligned} \mathrm{d}\Omega_{x_i} &= \sin\theta_{x_i}\,\mathrm{d}\theta_{x_i}\,\mathrm{d}\phi_{x_i}\,, \\ \mathrm{d}\Omega_{y_i} &= \sin\theta_{y_i}\,\mathrm{d}\theta_{y_i}\,\mathrm{d}\phi_{y_i}\,. \end{aligned} \qquad (7)$$

In terms of the hyperspherical variables, the Schrödinger equation becomes

$$\left[-\frac{\hbar^2}{2\mu}\left\{\frac{1}{\rho^5}\frac{\partial}{\partial\rho}(\rho^5\frac{\partial}{\partial\rho}) - \frac{\hat{\mathcal{K}}^2(\Omega_i)}{\rho^2}\right\} + V(\rho,\Omega_i) - E\right]\Psi(\rho,\Omega_i) = 0, \qquad (8)$$

where $V(\rho,\Omega_i) = V_{jk}(\vec{x}_i) + V_{ki}(\vec{x}_i,\vec{y}_i) + V_{ij}(\vec{x}_i,\vec{y}_i)$ is the total interaction potential expressed in terms of the hyperspherical variables and $\hat{\mathcal{K}}^2(\Omega_i)$ is the square of hyper-angular-momentum operator given by [52]

$$\hat{\mathcal{K}}^2(\Omega_i) = -\frac{\partial^2}{\partial{\phi_i}^2} - 4\cot 2\phi_i\,\frac{\partial}{\partial\phi_i} + \frac{1}{\cos^2\phi_i}\hat{l}^2(\hat{x}_i) + \frac{1}{\sin^2\phi_i}\hat{l}^2(\hat{y}_i), \qquad (9)$$

where $\hat{l}^2(\hat{x}_i)$ and $\hat{l}^2(\hat{y}_i)$ are the squares of ordinary orbital angular-momentum operators associated with $\vec{x}_i$ and $\vec{y}_i$ motions. The operator $\hat{\mathcal{K}}^2$ satisfies an eigenvalue equation [52]

$$\hat{\mathcal{K}}^2(\Omega_i)\mathcal{Y}_{K\alpha_i}(\Omega_i) = K(K+4)\mathcal{Y}_{K\alpha_i}(\Omega_i), \qquad (10)$$

where α_i is an abbreviation for the set of four quantum numbers $\{l_{x_i}, l_{y_i}, L, M\}$ and K, the hyper-angular-momentum quantum number (which is not a conserved quantity for the 3-body system), is given by $K = 2n_i + l_{x_i} + l_{y_i}$ (n_i being a non-negative integer). The quantity K is the degree of the homogeneous harmonic polynomials $\rho^K \mathcal{Y}_{K\alpha_i}(\Omega_i)$ in the Cartesian components of $\vec{x}_i$ and $\vec{y}_i$. Note that the quantum number K is invariant under the change of partition and hence does not involve the partition label. The eigenfunctions of $\hat{\mathcal{K}}^2$ are called hyperspherical harmonics (HH) and are given by

$$\mathcal{Y}_{K\alpha_i}(\Omega_i) = {}^{(2)}P_K^{l_{y_i}\ l_{x_i}}(\phi_i)\left[Y_{l_{x_i}}(\hat{x}_i)\ Y_{l_{y_i}}(\hat{y}_i)\right]_{LM}, \tag{11}$$

where

$${}^{(2)}P_K^{l_{y_i}\ l_{x_i}}(\phi_i) = N_K^{l_{x_i},\ l_{y_i}}\ (\cos\ \phi_i)^{l_{x_i}}\ (\sin\ \phi_i)^{l_{y_i}}\ P_{n_i}^{l_{y_i}+1/2,\ l_{x_i}+1/2}\ (\cos\ 2\phi_i). \tag{12}$$

The normalization constant $N_K^{l_{x_i},l_{y_i}}$ is given by

$$N_K^{l_{x_i},L_{y_i}} \ = \ \left[\frac{2\ n_i!(K+2)(n_i\ +\ l_{x_i}\ +\ l_{y_i}\ +\ 1)!}{\Gamma(n_i\ +\ l_{x_i}\ +\ 3/2)\ \Gamma(n_i\ +\ l_{y_i}+3/2)}\right]^{\frac{1}{2}} \tag{13}$$

and $P_n^{\alpha,\beta}(x)$ is the Jacobi polynomial [59]. The HH's $\{\mathcal{Y}_{K\alpha_i}(\Omega_i)\}$ form a complete orthonormal set in the angular hyperspace (Ω_i).

In the present method, the wave function $\Psi(\rho,\Omega_i)$ is expanded in the complete set of HH corresponding to a given partition (say partition 'i')

$$\Psi(\rho,\Omega_i) = \sum_{K\alpha_i} \frac{U_{K\alpha_i}(\rho)}{\rho^{5/2}} \mathcal{Y}_{K\alpha_i}(\Omega_i). \tag{14}$$

The factor $\rho^{-5/2}$ is included in order to remove the first-order derivative with respect to ρ in Eq. (8). Substitution of Eq. (14) in Eq. (8) and the use of orthonormality of HH leads to a set of coupled differential equations (CDE) in ρ

$$\begin{aligned} &\left[-\frac{\hbar^2}{2\mu}\left(\frac{\mathrm{d}^2}{\mathrm{d}\mathrm{d}\rho^2} - \frac{\mathcal{L}_K(\mathcal{L}_K+1)}{\rho^2}\right) - E\right] U_{K\alpha_i}(\rho) \\ + \quad &\textstyle\sum_{K'\alpha_i{}'} \langle K\alpha_i \mid V(\rho,\Omega_i) \mid K'\alpha_i{}'\rangle U_{K'\alpha_i{}'}(\rho) \ = \ 0, \end{aligned} \tag{15}$$

where $\mathcal{L}_K = K + 3/2$ and

$$\langle K\alpha_i|V(\rho,\Omega_i)|K'\alpha_i{}'\rangle = \int_{\Omega_i} \mathcal{Y}^*_{K\alpha_i}(\Omega_i)V(\rho,\Omega_i)\mathcal{Y}_{K'\alpha_i{}'}(\Omega_i)\ \mathrm{d}\Omega_i. \tag{16}$$

Since the expansion (14) is, in principle, an infinite one, the CDE, Eq. (15) are also an infinite set. For practical purposes, the expansion (14) has to be truncated to a finite set, leading to a finite set of CDE. Restrictions arising out of the symmetry requirement and imposition of conserved quantum numbers (e.g., total angular momentum, parity etc.) can reduce the expansion basis further and consequently a smaller set of CDE is to be solved.

Evaluation of the matrix elements of the type $\langle \mathcal{Y}_{K\alpha_i}(\Omega_i) \mid V_{jk}(x_i) \mid \mathcal{Y}_{K'\alpha_i{}'}(\Omega_i)\rangle$ (for central interactions) are straightforward, while those for the matrix elements of the type $\langle \mathcal{Y}_{K\alpha_i}(\Omega_i) \mid V_{ki}(x_j)|\mathcal{Y}_{K'\alpha_i{}'}(\Omega_i)\rangle$ and $\langle \mathcal{Y}_{K\alpha_i}(\Omega_i) \mid V_{ij}(x_k) \mid \mathcal{Y}_{K'\alpha_i{}'}(\Omega_i)\rangle$ become very complicated even for central interactions, since both $\vec{x}_j$ or $\vec{x}_k$ are expressed as linear combinations of $\vec{x}_i$ and $\vec{y}_i$, hence $\vec{x}_j$ and $\vec{x}_k$ depend on the polar angles of $\vec{x}_i$ and $\vec{y}_i$ (i.e. $\hat{x}_i$, $\hat{y}_i$) (see Eq. (2)). But the calculation of these matrix elements will be quite simple in the partitions 'j' or 'k', since in these partitions $\vec{x}_j$ or $\vec{x}_k$ are independent of $\vec{y}_j$ and $\vec{y}_k$, respectively. Since the choice of a particular partition is arbitrary, the HH basis corresponding to any chosen partition 'i' forms a complete set spanning the same hyperangular space. One can then relate the HH basis for two different partitions 'i' and 'j' through a unitary transformation. Then, a particular element $\mathcal{Y}_{K\alpha_i}(\Omega_i)$ in the partition 'i' can be expanded in the HH basis corresponding to partition 'j' as

$$\mathcal{Y}_{K\alpha_i}(\Omega_i) \;=\; \sum_{l_{x_j} l_{y_j}} \langle l_{x_i} l_{y_i} \mid l_{x_j} l_{y_j}\rangle_{KL} \mathcal{Y}_{K\alpha_j}(\Omega_j), \tag{17}$$

where the transformation coefficients $\langle l_{x_i} l_{y_i} \mid l_{x_j} l_{y_j}\rangle_{KL}$ are called the Raynal Revai coefficients (RRC) [60]. Since K, L and M are independent of the partition, the sum is over l_{x_j} and l_{y_j} only, subject to the restrictions $\vec{l}_{x_i} + \vec{l}_{y_i} = \vec{L} = \vec{l}_{x_j} + \vec{l}_{y_j}$. These coefficients can be computed easily [34]. Since the RRC's do not involve 'ρ', they are calculated once only and stored. That reduces the CPU time significantly.

In terms of the RRC's, the matrix elements of V_{ki} in the partition 'i' can be writen as

$$\begin{aligned} \langle \mathcal{Y}_{K\alpha_i}(\Omega_i) \mid V_{ki}(x_j) \mid \mathcal{Y}_{K'\alpha_i{}'}(\Omega_i)\rangle \;&=\; \textstyle\sum_{l'_{x_j} l'_{y_j} l_{x_j} l_{y_j}} \langle l_{x_i} l_{y_i} \mid l_{x_j} l_{y_j}\rangle^*_{KL} \\ &\times\;\; \langle l'_{x_i} l'_{y_i} \mid l'_{x_j} l'_{y_j}\rangle_{K'L} \\ &\times\;\; \langle \mathcal{Y}_{K\alpha_j}(\Omega_j) \mid V_{ki}(x_j) \mid \mathcal{Y}_{K'\alpha_j{}'}(\Omega_j)\rangle\,. \end{aligned} \tag{18}$$

The matrix element on the right-hand side of Eq. (18) has the same form as the matrix element of V_{jk} in the partition 'i' (the preferred partition) and can be evaluated in a simple way. Thus computing the RRC's involved in Eq. (18), the matrix element of V_{ki} in the partition 'i' can be evaluated easily. Similar technique can be employed for the calculation of the matrix element of V_{ij}.

Calculation of the potential matrix elements in the preferred partition (in which the pair interaction potential is a function only of the corresponding $\vec{x}$ of the partition) can be further simplified by introducing a multipolar expansion [35] of the potential. For a matrix element in the preferred partition, say partition 'i', the potential $V_{jk}(x_i)$ is expanded in an appropriate subset of corresponding HH,

$$V_{jk}(x_i) = \sum_{K''\alpha''} v^{(jk)}_{K''\alpha''}(\rho)\mathcal{Y}_{K''\alpha''}(\Omega_i)\,, \tag{19}$$

where $v^{(jk)}_{K''\alpha''}(\rho)$ is called the potential multipole and can be evaluated by the use of orthonormality of HH

$$v^{(jk)}_{K''\alpha_i''}(\rho) = \int V_{jk}(x_i) \mathcal{Y}^*_{K''\alpha_i''}(\Omega_i) \, \mathrm{d}\Omega_i \,. \tag{20}$$

The matrix element thus becomes

$$\langle \mathcal{Y}_{K\alpha_i}(\Omega_i) \mid V_{jk}(x_i) \mid \mathcal{Y}_{K'\alpha_i{}'}(\Omega_i)\rangle = \sum_{K''\alpha_i''} v^{(jk)}_{K''\alpha_i''}(\rho) \langle K\alpha_i \mid K''\alpha_i'' \mid K'\alpha_i'\rangle \,, \tag{21}$$

where

$$\langle K\alpha_i \mid K''\alpha_i'' \mid K'\alpha_i'\rangle = \int \mathcal{Y}^*_{K\alpha_i}(\Omega_i) \mathcal{Y}_{K''\alpha_i''}(\Omega_i) \mathcal{Y}_{K'\alpha_i'}(\Omega_i) \, \mathrm{d}\Omega_i \tag{22}$$

are called the geometrical structure coefficients (GSC). They are independent of ρ and the interaction. Hence, these coefficients need to be calculated once only and stored resulting in a fast and efficient algorithm. The GSC's involved in Eq. (21) can be calculated by a standard numerical integration. However, they can be calculated in a very elegant manner [40] by using the completeness property of the HH basis. Finally, the set of CDE's Eq. (15) is to be solved numericaly subject to the appropriate boundary conditions to get the energy E and the partial waves $U_{K\alpha_i}(\rho)$.

3. Results and discussion

In the present calculation, we have taken the core to be structureless. Since the core (α particle) contains only nucleons and no Λ-particles, there is no symmetry requirements under exchange of the valence Λ-particles with the core nucleons. The only symmetry requirements are (i) antisymmetrization of the core wave function under exchange of the nucleons and (ii) antisymmetrization of the three-body wave function under exchange of the two Λ-particles. The former is implicitly taken care of in the choice of the α-particle as a building block. The latter is correctly incorporated by restricting the l_{x_1} values, as discussed in detail in the following. Thus, within the three-body model, the symmetry requirements are correctly satisfied without any approximation. The ground state of ${}_{\Lambda\Lambda}^{6}$He has a total angular momentum $J = 0$ and a positive parity. The possible total spin (S) of the three-body system ($\alpha + \Lambda + \Lambda$) can take two values, '0' or '1'. Thus the total orbital angular momentum L can be either 0 or 1 corresponding to $S = 0$ or 1, respectively. Hence the ground state of ${}_{\Lambda\Lambda}^{6}$He is an admixture of the states ${}^1\mathrm{S}_0$ and ${}^3\mathrm{P}_0$. However, for purely central spin-independent interactions (as used in this work), these states do not mix. In our case, the ground state of ${}_{\Lambda\Lambda}^{6}$He is a pure ${}^1S_0$ state. Since the α-particle is spinless, the spin singlet state ($S = 0$) corresponds to the zero total spin of the valence Λ-particles (i.e. S_{23}=0). Hence, the spin part of the wave function is antisymmetric under the exchange of the spins of the two Λ-particles. Thus the spatial part must be symmetric under the exchange of the two Λ-hyperons. The symmetry of the spatial part is determined by the hyperspherical harmonics, since the hyperradius ρ and hence the hyperradial partial waves ($U_{K\alpha}(\rho)$) are invariant under permutation of the particles. Under the pair exchange operator P_{23}, which interchanges particles 2 and 3, $\vec{x}_1 \to -\vec{x}_1$ XXX, and $\vec{y}_1$ remains unchanged (see Eq. (2)). Consequently, P_{23} acts like the parity operator for (23) pair only. Choosing the two valence Λ-hyperons to be in the spin singlet state (spin antisymmetric), the space wave function must be symmetric under P_{23}. This requires l_{x_1} to be even. For the spin singlet state, total orbital angular momentum $L = 0$, hence we must have $l_{x_1} = l_{y_1} =$ even integer. Since $K = 2n_1 + l_{x_1} + l_{y_1}$, where n_1 is a non-negative integer, K must be even and

$$\begin{array}{lllll} l_{x_1} & = & l_{y_1} & = & 0, 2, 4, \ldots, K/2 \qquad \text{if } K/2 \text{ is even} \\ & & & & 0, 2, 4, \ldots, K/2 - 1) \qquad \text{if } K/2 \text{ is odd} \end{array} \tag{23}$$

Again, for the triplet state ($S = 1$), the two valence Λ-hyperons will be in the spin triplet state ($S_{23} = 1$, spin symmetric). Hence, the space wave function must be antisymmetric under P_{23}. This then requires l_{x_1} to be odd. For the spin triplet state, the total orbital angular momentum, $L = 1$, hence l_{y_1} may take values l_{x_1} and $l_{x_1} \pm 1$, but the parity conservation allows $l_{y_1}{=}l_{x_1}$ only. Again, since $K = 2n_1 + l_{x_1} + l_{y_1}$, where n_1 is a non-negative integer, K must be even and

$$\begin{array}{lllll} l_{x_1} & = & l_{y_1} & = & 1, 3, 5, \ldots, K/2 \qquad \text{if } K/2 \text{ is odd} \\ & & & & 1, 3, 5, \ldots, K/2 - 1) \qquad \text{if } K/2 \text{ is even}\,. \end{array} \tag{24}$$

For a practical calculation, the HH expansion basis (Eq. (14)) is truncated to a maximum value ($K_{\max}$) of K. For each allowed $K \le K_{\max}$ with $K =$ even integers, all allowed values of l_{x_1} (according to Eq.(23) for spin-independent central interactions) are included. This truncates Eq. (15) to a set of N coupled differential equations, where

$$\begin{array}{lll} N & = & \left(\frac{1}{4}K_{\max} + 1\right)^2 \qquad \text{if } K_{\max}/2 \text{ is even} \\ & = & \left(\frac{1}{4}K_{\max} + \frac{1}{2}\right)\,\left(\frac{1}{4}K_{\max} + \frac{3}{2}\right) \qquad \text{if } K_{\max}/2 \text{ is odd}\,. \end{array} \tag{25}$$

The truncated set of CDE has been solved by the hyperspherical adiabatic approximation (HAA) [61].

3.1. Two-body potentials

We used the same two types of purely attractive one-term Gaussian $\alpha\Lambda$ potentials as used by Tang and Herndon [12] without any restriction over l values. The $\alpha\Lambda$ potentials are given by

type-A: $V^A_{\alpha\Lambda}(r) = V^A_0 \exp(-r^2/\chi^2_A)$ with $V^A_0 = -43.46$ MeV, $\chi_A = 1.578$ fm,

type-B: $V^B_{\alpha\Lambda}(r) = V^B_0 \exp(-r^2/\chi^2_B)$ with $V^B_0 = -60.17$ MeV, $\chi_B = 1.273$ fm.

The $\alpha\Lambda$ interaction is obtained by folding a Λ-nucleon potential into the nuclear density distribuion of α-particle which is chosen to have a Gaussian shape with a r.m.s. radius of 1.44 fm [12]. The first type (type-A) $\alpha\Lambda$ potential is obtained with a purely attractive Λ-nucleon interaction of a Gaussian form having an intrinsic range of 1.5 fm. This $\alpha\Lambda$ potential reproduces the experimental value (3.04 MeV) for the binding energy of the Λ-particle in $^{5}_{\Lambda}$He [62]. The $\alpha\Lambda$ interaction of type-B is obtained by using a purely attractive Gaussian Λ-nucleon potential of intrinsic range 0.7 fm in the folding process [12]. A number of phenomenological as well as meson-exchange motivated forms were used for the $\Lambda\Lambda$ interaction in earlier attempts. Based on the data available, some selection was made between Nijmegen potential models [63–64]. Since knowledge of the $\Lambda\Lambda$ scattering is still quite inadequate, it is not possible to establish a realistic $\Lambda\Lambda$ potential at this stage. Instead, we adopt here a purely phenomenological strategy. For the $\alpha\Lambda$ potential of the first type (type-A), the $\Lambda\Lambda$ potential is chosen to be a two term l independent Gaussian, having a short range repulsive part and a longer range attractive part, of the form

$$V_{\Lambda\Lambda}(r) = V_r \exp(-r^2/b_r^2) - V_a \exp(-r^2/b_a^2). \tag{26}$$

We choose the parameters such that the observables of ${}_{\Lambda\Lambda}^{6}$He are close to the known values. This gives $V_r = 800$ MeV, $b_r = 0.4$ fm and $V_a = 474$ MeV, $b_a = 0.58$ fm. For the type-B $\alpha\Lambda$ interaction, we used a slightly modified $\Lambda\Lambda$ interaction of the same form but with parameters $V_r = 800$ MeV, $b_r = 0.4$ fm and $V_a = 447.5$ MeV, $b_a = 0.58$ fm. As evident from Eq. (25), the number of basis states and hence the size of CDE increases rapidly as $K_{\max}$ increases. The truncated set of CDE takes the form

$$\begin{aligned}&\left[-\frac{\hbar^2}{2\mu}\left(\frac{\mathrm{d}^2}{\mathrm{d}\rho^2} - \frac{\mathcal{L}_K(\mathcal{L}_K+1)}{\rho^2}\right) - E\right] U_{Kl_{x_1}LS}(\rho) \\ &+ \sum_{K'=0,2,\ldots}^{K_{\max}} \sum_{l'_{x_1}\,(\text{allowed})} \langle K l_{x_1} \mid V(\rho,\Omega_1) \mid K' l'_{x_1}\rangle U_{K' l'_{x_1} LS}(\rho) \;=\; 0\end{aligned} \tag{27}$$

(allowed l'_{x_1}=0, 2, ...only for $S = 0, L = 0$). Note that the subscripts l_{y_1} (=l_{x_1}) or l'_{y_1} (=l'_{x_1}) have been suppressed for brevity. The calculated values of binding energy (BE) for various values of $K_{\max}$ up to 20 are shown for the ground state of ${}_{\Lambda\Lambda}^{6}$He treated as α+Λ+Λ, for type-A $\alpha\Lambda$ potential in Table 1 and for type-B $\alpha\Lambda$ potential in Table 2.

In Tables 1 and 2, $K_{\max}$ values are taken to be even integers, as required (see previous section). The differences in BE [$\Delta(BE) = BE(K_{\max}) - BE(K_{\max}-2)$] for different $K_{\max}$ are shown in the 3rd columns of Tables 1 and 2. The calculated binding energy $B_{\Lambda\Lambda}$ of ${}_{\Lambda\Lambda}^{6}$He agrees fairly well with the experimental value ((10.80$\pm$ 0.60) MeV) [2] within the experimental error limit.

Having obtained the wave function by the HH approach and assuming the same set of two body interactions, some of the observables of the three-body system have been calculated. These include the r.m.s. radius of ${}_{\Lambda\Lambda}^{6}$He

$$R_A = \left[\frac{A_c R_c^2 + m_\Lambda \langle r_{13}^2 + r_{12}^2\rangle}{A_c + 2m_\Lambda}\right]^{1/2}, \tag{28}$$

whereA_c, m_Λ are the masses of the core and the Λ-hyperon (in units of nucleon mass) and R_c is the matter radius of the core. For the ${}_{\Lambda\Lambda}^{6}$He (^{4}He+$\Lambda+\Lambda$)-system,

$A_c = 4$ and $R_c = 1.47$ fm [65]. The r.m.s. $\alpha\Lambda$ separation is defined as

$$R_{\alpha\Lambda} = \left[\frac{1}{2}\langle r_{13}^2 + r_{12}^2\rangle\right]^{1/2}. \tag{29}$$

Table 1. Calculated BE $B_{\Lambda\Lambda}$ for different $K_{\max}$ values for type-A $\alpha\Lambda$ potential.

$K_{\max}$	BE (MeV)	$\Delta(BE)$ MeV
0	09.79427	
2	10.05604	0.26177
4	10.50092	0.44488
6	10.60920	0.10828
8	10.67141	0.06221
10	10.71487	0.04346
12	10.74764	0.03277
14	10.77131	0.02367
16	10.78781	0.01650
18	10.79901	0.01120
20	10.80649	0.00748

Table 2. Calculated BE $B_{\Lambda\Lambda}$ for different $K_{\max}$ values for type-B $\alpha\Lambda$ potential.

$K_{\max}$	BE (MeV)	$\Delta(BE)$ (MeV)
0	09.70729	
2	09.86155	0.15126
4	10.48417	0.62262
6	10.60990	0.12573
8	10.68669	0.07679
10	10.73439	0.04770
12	10.76657	0.03218
14	10.78820	0.02173
16	10.80178	0.01358
18	10.81038	0.00860
20	10.81581	0.00543

The expectation value of the observables $\langle r_{13}^2 + r_{12}^2\rangle$ are obtained by the expression

$$\langle r_{13}^2 + r_{12}^2\rangle = \sum_{KK'l_{x_1}LS} \int_0^\infty \rho^2 \mathrm{d}\rho\, U_{Kl_{x_1}LS}(\rho) U_{K'l_{x_1}LS}(\rho) \tag{30}$$

$$\times \int_0^{\pi/2} {}^{(2)}P_K^{\,l_{x_1},l_{x_1}}(\phi)\ {}^{(2)}P_{K'}^{\,l_{x_1},l_{x_1}}(\phi) \left[\sqrt{\frac{5}{8}}\cos^2\phi + \sqrt{\frac{8}{5}}\ \sin^2\phi\right] \cos^2\phi \sin^2\phi\, \mathrm{d}\phi.$$

The r.m.s. separation between the valence Λ-hyperons ($R_{\Lambda\Lambda}$) is given by the expression

$$R_{\Lambda\Lambda} = \sqrt{\langle r_{23}^2\rangle}\,, \tag{31}$$

where

$$\begin{aligned}\langle r_{23}^2\rangle &= \sqrt{\tfrac{5}{2}} \textstyle\sum_{KK'l_{x_1}LS} \displaystyle\int_0^\infty \rho^2 \mathrm{d}\rho U_{Kl_{x_1}LS}(\rho) U_{K'l_{x_1}LS}(\rho) \\ &\times \int_0^{\pi/2} {}^{(2)}P_K^{\,l_{x_1},l_{x_1}}(\phi)\ \ {}^{(2)}P_{K'}^{\,l_{x_1},l_{x_1}}(\phi) \cos^4\phi \sin^2\phi\, \mathrm{d}\phi\,.\end{aligned} \tag{32}$$

The r.m.s. separation between the core (α) and the C.M. of $\Lambda\Lambda$ pair is given by the expression

$$R_{(\Lambda\Lambda)c} = \sqrt{\langle r^2_{(23)1} \rangle}\,, \tag{33}$$

where

$$\begin{aligned} \langle r^2_{(23)1} \rangle \;&=\; \sqrt{\tfrac{2}{5}} \textstyle\sum_{KK'l_{x_1}LS} \displaystyle\int_0^\infty \rho^2 \mathrm{d}\rho\; U_{Kl_{x_1}LS}(\rho)\; U_{K'l_{x_1}LS}(\rho) \\ &\times \int_0^{\pi/2} {}^{(2)}P_K^{\,l_{x_1},l_{x_1}}(\phi)\; {}^{(2)}P_{K'}^{\,l_{x_1},l_{x_1}}(\phi)\; \cos^2\phi\; \sin^4\phi\; \mathrm{d}\phi\,. \end{aligned} \tag{34}$$

We then calculated the ratio $R_{\Lambda\Lambda}/R_{(\Lambda\Lambda)\mathrm{c}}$ to compare it with the results of a three-body ${}^{A}Z + \Lambda + \Lambda$ calculation by Yamamoto et al. [67] with finite range $\Lambda\Lambda$ potential with a repulsive core. The computed values of these observables for various $K_{\max}$ are shown in Tables 3 and 4. The binding energy and some other observables computed by Ikeda et al. [16] is shown in Table 5.

Table 3. Calculated observables for ${}^{6}_{\Lambda\Lambda}$He *for different* $K_{\max}$ *values for type-A* $\alpha\Lambda$ *potential.*

$K_{\max}$	R_A(matter) (fm)	$R_{\alpha\Lambda}$ (fm)	$R_{\Lambda\Lambda}$ (fm)	$R_{(\Lambda\Lambda)c}$ (fm)	$\frac{R_{\Lambda\Lambda}}{R_{(\Lambda\Lambda)c}}$	η
0	1.6948	2.0171	2.5019	1.5824	1.5811	0.3162
2	1.6850	1.9948	2.5198	1.5466	1.6293	0.3198
4	1.6984	2.0251	2.5399	1.5774	1.6102	0.3221
6	1.6984	2.0251	2.5418	1.5766	1.6122	0.3224
8	1.6982	2.0247	2.5358	1.5786	1.6064	0.3231
10	1.6972	2.0225	2.5313	1.5776	1.6045	0.3234
12	1.6965	2.0209	2.5277	1.5769	1.6030	0.3238
14	1.6960	2.0199	2.5251	1.5766	1.6016	0.3241
16	1.6958	2.0193	2.5234	1.5766	1.6005	0.3242
18	1.6957	2.0190	2.5222	1.5767	1.5997	0.3244
20	1.6957	2.0190	2.5215	1.5770	1.5989	0.3246

Finally, in order to study the correlation among the constituent particles (i.e. the α-core and the valence Λ-hyperons), we computed the probability density $P(r_{\Lambda\Lambda}, r_{(\Lambda\Lambda)c})$, where $r_{\Lambda\Lambda} = \left[(m_1(m_2+m_3)^2)/(m_2 m_3 M)\right]^{1/4} x_1$ and $r_{(\Lambda\Lambda)c} = \left[(m_2 m_3 M)/(m_1(m_2+m_3)^2)\right]^{1/4}\; y_1$ (see Eq. (2)) are, respectively, the separation between the valence Λ-hyperons and the separation of the core from the centre of mass of the valence Λ-hyperons. The probability density is defined as the

Table 4. Calculated observables for $^{6}_{\Lambda\Lambda}$He *for different* $K_{\max}$ *values for type-B* $\alpha\Lambda$ *potential.*

$K_{\max}$	R_A(matter) (fm)	$R_{\alpha\Lambda}$ (fm)	$R_{\Lambda\Lambda}$ (fm)	$R_{(\Lambda\Lambda)c}$ (fm)	$\frac{R_{\Lambda\Lambda}}{R_{(\Lambda\Lambda)c}}$	η
0	1.6160	1.8356	2.2767	1.4399	1.5811	0.3162
2	1.6100	1.8215	2.3117	1.4078	1.6421	0.3133
4	1.6239	1.8540	2.3380	1.4391	1.6246	0.3152
6	1.6239	1.8541	2.3432	1.4370	1.6314	0.3149
8	1.6241	1.8550	2.3393	1.4391	1.6255	0.3155
10	1.6232	1.8525	2.3362	1.4379	1.6247	0.3159
12	1.6227	1.8514	2.3335	1.4374	1.6245	0.3161
14	1.6225	1.8507	2.3318	1.4373	1.6223	0.3164
16	1.6224	1.8505	2.3307	1.4374	1.6215	0.3165
18	1.6224	1.8505	2.3300	1.4477	1.6206	0.3167
20	1.6224	1.8505	2.3296	1.4479	1.6201	0.3168

Table 5. Calculated observables for $^{6}_{\Lambda\Lambda}$He *system by K. Ikeda et al. 16].*

BE (MeV)	R_A(matter) (fm)	$R_{\Lambda\Lambda}$(fm)	$R_{(\Lambda\Lambda)c}$(fm)
10.80	1.58	2.52	1.60

probability of finding the three-body system having definite separations between the constituent particles. This probability density is given by the expression

$$P(r_{\Lambda\Lambda}, r_{(\Lambda\Lambda)c}) \tag{35}$$
$$= \sum_{KK'l_{x_1}LS} U_{Kl_{x_1}LS}(\rho) U_{K'l_{x_1}LS}(\rho) {}^{(2)}P_K^{l_{x_1},l_{x_1}}(\phi) {}^{(2)}P_{K'}^{l_{x_1},l_{x_1}}(\phi) \cos^2\phi \sin^2\phi \,,$$

with

$$\rho = \left[\sqrt{\frac{2}{5}}\, r_{\Lambda\Lambda}^2 + \sqrt{\frac{5}{2}}\, r_{(\Lambda\Lambda)c}^2 \right]^{1/2} \tag{36}$$

and

$$\phi = \tan^{-1}\left(\sqrt{\frac{5}{2}}\, \frac{r_{(\Lambda\Lambda)c}}{r_{\Lambda\Lambda}} \right) . \tag{37}$$

A three-dimensional plot of $P(r_{\Lambda\Lambda}, r_{(\Lambda\Lambda)c})$ as a function of $r_{\Lambda\Lambda}$ and $r_{(\Lambda\Lambda)c}$ is displayed in Figs. 2a and b for the type-A and type-B $\alpha\Lambda$ potentials, respectively. The

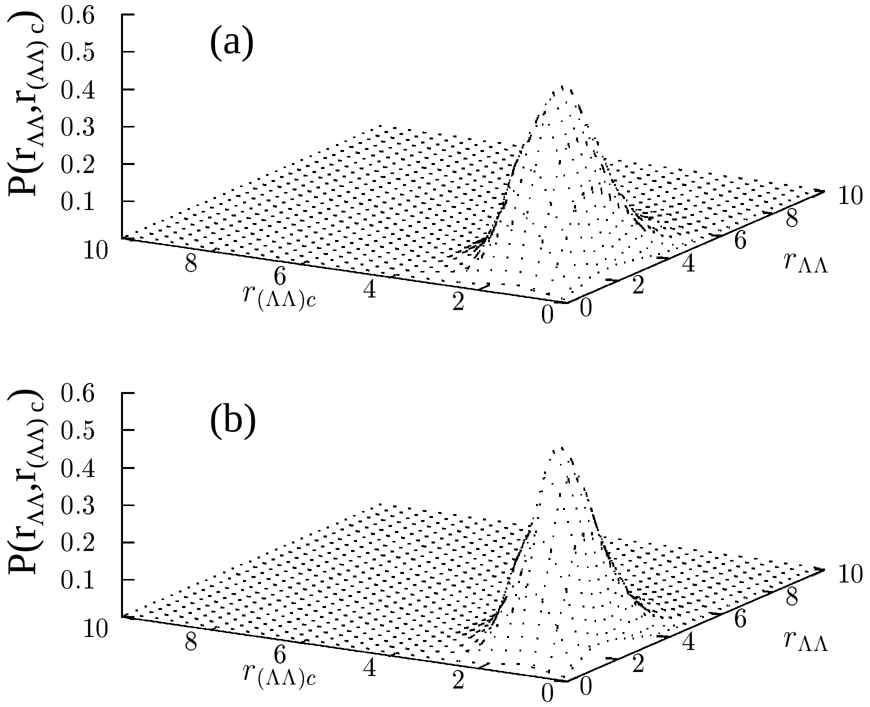

Fig. 2. Correlation density plot for the ground state of $^{6}_{\Lambda\Lambda}$He *in the* $\Lambda\Lambda$ *and* $(\Lambda\Lambda)c$ *variables (in* fm*) a) for type-A* $\alpha\Lambda$ *potential and b) for type-B* $\alpha\Lambda$ *potential.*

density plot exhibits a cigar-like shape where the valence Λ-hyperons are located on opposite side of the α-core ($r_{\Lambda\Lambda} > r_{(\Lambda\Lambda)c}$). This can further be confirmed by computing a correlation coefficient defined as

$$
\begin{aligned}
\eta &= \langle \frac{r^2_{(\Lambda\Lambda)c}}{\rho^2} \rangle \\
&= \sqrt{\tfrac{2}{5}} \textstyle\sum_{KK'l_{x_1}LS} \displaystyle\int_0^\infty \mathrm{d}\rho \; U_{Kl_{x_1}LS}(\rho) \; U_{K'l_{x_1}LS}(\rho) \\
&\times \int_0^{\pi/2} {}^{(2)}P_K{}^{l_{x_1},l_{x_1}}(\phi) \; {}^{(2)}P_{K'}{}^{l_{x_1},l_{x_1}}(\phi) \\
&\times \cos^2\phi \sin^4\phi \; \mathrm{d}\phi.
\end{aligned} \tag{38}
$$

A small value of this coefficient will indicate that the two valence Λ-hyperons are situated on opposite sides of the α-core (i.e., a cigar shape where the Λ-hyperons are anti-correlated). A large value ($\eta \leq 1$) will indicate the possibility of $\Lambda - \Lambda$ correlation.

The computed values of this coefficient for various $K_{\max}$ are shown in the last columns of Tables 3 and 4. As the value of η is small (≈ 0.32), a cigar shape is indicated on the average. Thus, the correlation density plots (Figs. 2a and b) and the computed value of the correlation coefficient η both indicate that the cigar-like structures are probable. In addition to the above, we also calculated the BE, the r.m.s. matter radii, the correlation coefficient (η), the partial probability (P_l) and plotted the probability density to compare our calculation with those of Ikeda et al. [16], using the same potential model as used by Ikeda. They assumed the ΛN and ΛΛ interactions to be central with a simple Gaussian form [13]

$$V(r) = V^0 \exp(-r^2/\beta^2)\,.$$
$$\Lambda\mathrm{N}: \quad V^0 = -38.19 \ \ \mathrm{MeV}, \quad \beta = 1.034 \ \mathrm{fm}$$
$$\Lambda\Lambda: \quad V^0 = -52.25 \ \ \mathrm{MeV}, \quad \beta = 1.034 \ \mathrm{fm}.$$

The ΛN interaction folded with Φ_α (^{4}He core wave function) gives the $\Lambda\alpha$ potential $V_{\Lambda\alpha}(r)$,

$$\Lambda\alpha: \quad V^0 = -64.20 \ \mathrm{MeV}, \quad \beta = 1.173 \ \mathrm{fm}.$$

For various $K_{\max}$ values, the binding energies are listed in Table 6, the r.m.s. radii and the correlation coefficient are listed in Table 7 while the partial probabilities are listed in Table 8. The probabilty density distribution is depicted in Fig. 3. If we now make a comparison of the results obtained in the present calculation (see Table 6) and those obtained by Ikeda et al. (see Table 5), we immediately find that

Table 6. Calculated BE $B_{\Lambda\Lambda}$ for different $K_{\max}$ values for potential model of Ikeda et al. [16].

$K_{\max}$	BE (MeV)	Δ(BE) MeV
0	9.85620	
2	9.92450	0.06830
4	10.53343	0.60893
6	10.59943	0.06600
8	10.62321	0.02378
10	10.62669	0.00348
12	10.62813	0.00144
14	10.62864	0.00051
16	10.62879	0.00015
18	10.62885	0.00006
20	10.62888	0.00003

Table 7. Calculated observables for ${}^{6}_{\Lambda\Lambda}$He for different $K_{\max}$ values for potential model of Ikeda et al. [16].

$K_{\max}$	R_A(matter) (fm)	$R_{\alpha\Lambda}$ (fm)	$R_{\Lambda\Lambda}$ (fm)	$R_{(\Lambda\Lambda)c}$ (fm)	$\frac{R_{\Lambda\Lambda}}{R_{(\Lambda\Lambda)c}}$	η
0	1.5855	1.7627	2.1863	1.3828	1.5811	0.3142
2	1.5837	1.7583	2.1888	1.3761	1.5906	0.3201
4	1.5971	1.7906	2.2181	1.4058	1.5778	0.3218
6	1.5995	1.7964	2.2284	1.4091	1.5814	0.3215
8	1.6017	1.8016	2.2300	1.4160	1.5749	0.3219
10	1.6021	1.8025	2.2309	1.4160	1.5750	0.3219
12	1.6024	1.8031	2.2310	1.4167	1.5748	0.3221
14	1.6025	1.8034	2.2310	1.4170	1.5747	0.3221
16	1.6025	1.8035	2.2310	1.4171	1.5746	0.3221
18	1.6025	1.8035	2.2310	1.4170	1.5747	0.3221
20	1.6025	1.8036	2.2310	1.4172	1.5742	0.3221

Table 8. Calculated Contribution of various orbital angular momenta to the probability distribution of ${}^{6}_{\Lambda\Lambda}$He for potential model of Ikeda et al. [16] ($l = l_{x_1} = l_{y_1}$).

$K_{\max}$	Partial probability (P_l)		
	$l=0$	$l=2$	$l=4$
0	1.0000	0.0000	0.0000
2	1.0000	0.0000	0.0000
4	0.9932	0.0068	0.0000
6	0.9930	0.0070	0.0000
8	0.9929	0.0070	0.0001
10	0.9929	0.0070	0.0001
12	0.9929	0.0070	0.0001
14	0.9929	0.0070	0.0001
16	0.9929	0.0070	0.0001
18	0.9929	0.0070	0.0001
20	0.9929	0.0070	0.0001

the binding energy converges nicely at $K_{\max} = 20$. However, one may notice that the fully converged value of the BE is slightly less than that obtained by Ikeda et al. This discrepancy in the binding energy may have arisen due to the different choice of masses of the system particles. It is true that the restriction to $l = 4$ ($l = l_{x_1} = l_{y_1}$) does not lead to any significant effect to the partial probability (see Table 8), but it leads to a small increment (≈ 0.005 MeV) in the binding energy (see Table 6). The values of the calculted r.m.s. matter radius R_A (see column 2 of Table 7) do not differ much from those obtained by Ikeda et al. (see Table 5), however, other observables differ slightly. These small differences may be due to the different theoretical method used by Ikeda et al.

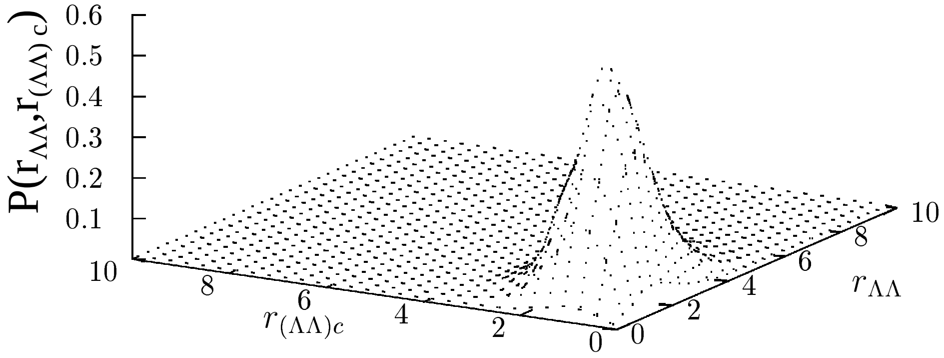

Fig. 3 Correlation density plot for the ground state of ${}^{6}_{\Lambda\Lambda}$He *in the* $\Lambda\Lambda$ *and* $(\Lambda\Lambda)c$ *variables (in* fm*) for potential model of Ikeda et al. [16].*

4. Conclusion

The hyperspherical harmonics expansion (HHE) method adopted here is an essentially exact method, where calculations can be carried out up to any desired precision. This can be seen in Tables 1 – 4, 6 and 7. As is evident from Tables 1 and 2, the convergence of the binding energy (with respect to increasing $K_{\max}$) is relatively slow, whereas the convergence rate for the other observables (Tables 3 and 4) are faster. The observed ground state binding energies of the nuclei ${}^{6}_{\Lambda\Lambda}$He, ^{6}He(α+n+n) and ^{6}Li(α+n+p) are (10.80$\pm$0.60) MeV [2], (0.973$\pm$0.04) MeV [65] and 3.672 MeV [66], respectively. At present, we have no experimental data for the r.m.s. matter radius of ${}^{6}_{\Lambda\Lambda}$He to compare with our calculated result. But the relatively large value of the binding energy of ${}^{6}_{\Lambda\Lambda}$He indicates that it is more compact than the ^{6}He(α+n+n) and ^{6}Li(α+n+p) systems. This in turn demands that the r.m.s. matter radius of ${}^{6}_{\Lambda\Lambda}$He should have a smaller value compared to that for ^{6}He and ^{6}Li nuclei. The observed matter radii for ^{6}He and ^{6}Li are respectively (2.57 ± 0.10) fm [65] and (2.56 ± 0.05) fm [66] which are larger than the matter radii (R_A) calculated by us (see Tables 3 and 4) and by Ikeda et al. (see Table 5) for the ground state of ${}^{6}_{\Lambda\Lambda}$He. This agrees with the foregoing remark. A relatively small value (≈ 0.32) (see Tables 3 and 4) of the calculated correlation coefficient indicates that the valence hyperons are not correlated. A comparision of

Tables 3 and 4 with Table 5 shows that the calculated value of the r.m.s. matter radius (R_A(matter)) for type-B $\alpha\Lambda$ potential agrees fairly well with that calculated by Ikeda et al., while the r.m.s. $R_{(\Lambda\Lambda)c}$ and $R_{\Lambda\Lambda}$ radii agree with those for type-A of $\alpha\Lambda$ potential. The calculated value of the ratio $R_{\Lambda\Lambda}/R_{(\Lambda\Lambda)c}$ (see Tables 3 and 4) for both types of $\alpha\Lambda$ potentials used here are quite close to the value (1.53) obtained by Yamamoto et al. [67]. The reliability of the HHE method

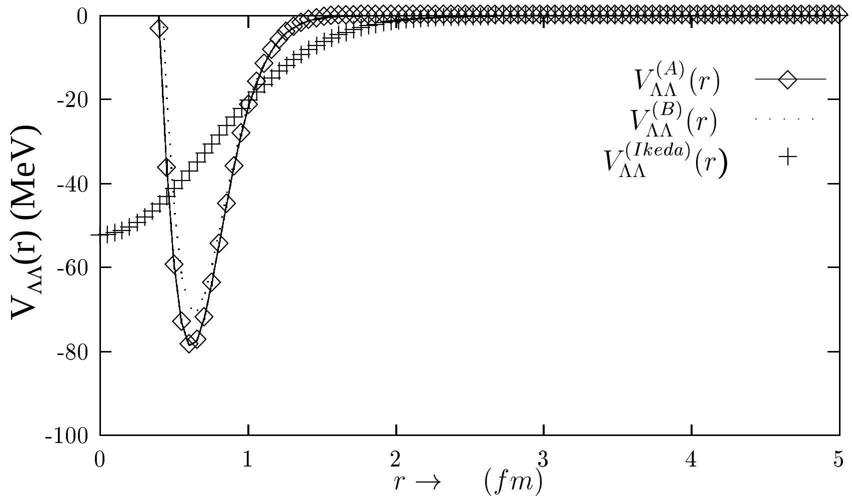

Fig. 4 Plot of the type-A, type-B and Ikeda's [16] $\Lambda\Lambda$ *potentials.*

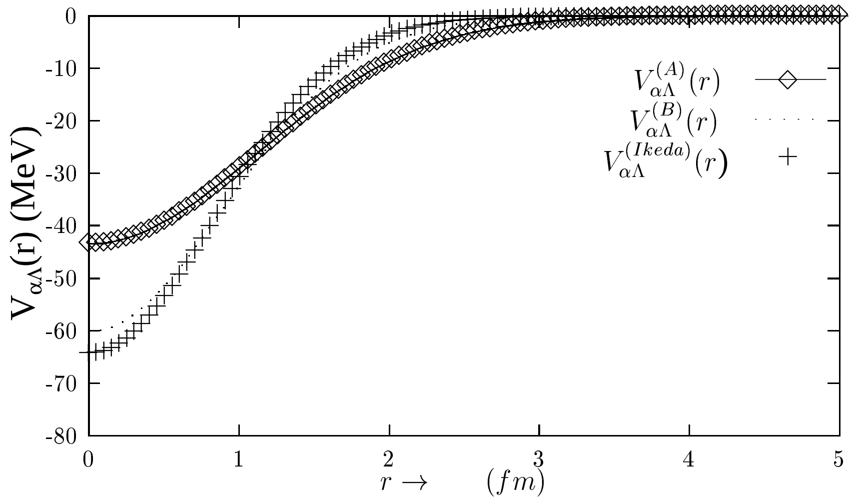

Fig. 5 Plot of the type-A, type-B and Ikeda's [16] $\alpha\Lambda$ *potentials.*

lends credence to the information sought about the $\alpha\Lambda$ and $\Lambda\Lambda$ potentials from the bound state properties of ${}^{6}_{\Lambda\Lambda}$He. A number of $\alpha\Lambda$ and $\Lambda\Lambda$ potentials have already been used in the literature [12,16]. The results of calculations by Ikeda et al [16] seem to be closer to the experimental value of BE and various radii expected from phenomenological arguments. However, although one does not expect a repulsive core in the $\alpha\Lambda$ potential (since α contains no Λ-particles and the Pauli repulsive core should be absent), one infact can expect a strongly repulsive core in the $\Lambda\Lambda$ potential. In the potential model proposed by Ikeda et al., there is no repulsive core in the $\Lambda\Lambda$ potential. Hence, we slightly modified the potential model of Tang and Herndon [12] to include a soft repulsive core in the $\Lambda\Lambda$ potential, in both models A and B. We have verified that the $\alpha\Lambda$ potential chosen here reproduce the binding energy of the Λ-particle in ${}^{5}_{\Lambda}$He correctly. As discussed above, both produce BE within experimental error limits and important radii within experimental range. Out of these, the potential model-B appears to produce results closer to those of Ikeda et al. In Figs. 4 and 5, we compare the $\alpha\Lambda$ and $\Lambda\Lambda$ potentials of all three models. Since our model-B produces experimental results for ${}^{6}_{\Lambda\Lambda}$He and also has a soft repulsive core in the $\Lambda\Lambda$ potential, we conclude that this one is a better potential model for the $\alpha\Lambda$ and $\Lambda\Lambda$ interactions.

Acknowledgements

Part of the calculation was done on computers provided by the Departmental Special Assistance (DSA) of the University Grants Commission (UGC), India.

References

[1] M. Danysz et al., Nucl. Phys. **49** (1963) 121.

[2] J. Prowse, Phys. Rev. Lett. **17** (1966) 782.

[3] R. H. Dalitz, D. H. Davis, P. H. Fowler, A. Montwill, J. Poriewski and J. A. Zakrzewski, Proc. R. Soc. (London) A **426** (1989) 1.

[4] S. Aoki et al., Prog. Theo. Phys. **85** (1991) 1287.

[5] A. Gal, Adv. Nucl. Phys., eds. M. Baranger and E. Vogt, **8** (1975) 1.

[6] G. Alexander et al., Phys. Rev. **173** (1968) 1452.

[7] B. Sechi-Zorn et al., Phys. Rev. **175** (1968) 1735.

[8] J. A. Kadyk et al., Nucl. Phys. **B27** (1971) 13.

[9] J. M. Hauptman, LBL Report No. 3608 (1974).

[10] F. Eisele et al., Phys. Lett. B **37** (1971) 204.

[11] R. Engelmann et al., Phys. Lett. **21** (1966) 487.

[12] Y. C. Tang and R. C. Herndon, Nuovo Cimento B **56** (1966) 117.

[13] R. H. Dalitz and G. Rajasekaran, Nucl. Phys. **50** (1964) 450.

[14] A. R. Ali and A. R. Bodmer, Phys. Lett. B **24** (1967) 343.

[15] A. R. Bodmer, Q. N. Usmani and J. Carlson, Nucl. Phys. A **422** (1984) 510.

[16] K. Ikeda, H. Bando and T. Motoba, Prog. Theo. Phys. Suppl. **81** (1985) 147.

[17] C. D. Lin, Phys. Rep. **257** (1995) 1.

[18] T. H. Gronwall, Phys. Rev. **51** (1937) 655.

[19] C. D. Lin, Phys. Rev. A **29** (1984) 1019.

[20] C. D. Lin, Phys. Rev. Lett. **51** (1983) 1348.

[21] J. Macek, J. Phys. B **1** (1968) 831.

[22] C. H. Greene, Phys. Rev. A **23** (1981) 661.

[23] C. D. Lin and Xian- Hui Liu, Phys. Rev. A **37** (1988) 2749.

[24] H. Fakuda, T. Ishihura and S. Hara, Phys. Rev. A **41** (1990) 1455.

[25] A. M. Launay and M. Le Dourneuf, J. Phys. B **15** (1982) 455.

[26] J. L. Ballot and J. Navarro, J. Phys. B **8** (1975) 172.

[27] R. C. Whitten and J. S. Sims, Phys. Rev. A **9** (1974) 1586.

[28] R. M. Shoucri and B. T. Darling, Phys. Rev. A **12** (1987) 2272.

[29] V. B. Mandelzweig, Phys. Lett. A **78** (1980) 25.

[30] V. D. Efros, A. M. Frolov and M. I. Mukhtarova, J. Phys. B **15** (1982) 1819.

[31] T. K. Das, R. Chattopadhyay and P. K. Mukherjee, Phys. Rev. A **50** (1994) 3521.

[32] R. Chattopadhyay, T. K. Das and P. K. Mukherjee, Physica Scripta **54** (1996) 601.

[33] R. Chattopadhyay and T. K. Das, Phys. Rev. A **57** (1997) 1281.

[34] Md. A. Khan, S. K. Datta and T. K. Das, Fizika B (Zagreb) **8** (1999) 469.

[35] T. K. Das, H. T. Coelho and M. Fabre de la Ripelle, Phys. Rev. C **26** (1982) 2288.

[36] H. T. Coelho, T. K. Das and M. Fabre de la Ripelle, Phys. Letts. B **109** (1982) 255.

[37] T. K. Das and H. T. Coelho, Phys. Rev. C **26** (1982) R754.

[38] T. K. Das and H. T. Coelho, Phys. Rev. C **26** (1982) 697.

[39] H. T. Coelho, T. K. Das and M. Robilotta, Phys. Rev. C **28** (1983) 1812.

[40] T. B. De and T. K. Das, Phys. Rev. C **36** (1987) 402.

[41] V. P. Brito, H. T. Coelho and T. K. Das, Phys. Rev. A **40** (1989) 3346.

[42] A. K. Ghosh and T. K. Das, Phys. Rev. C **42** (1990) 1249.

[43] T. K. Das and H. T. Coelho and J. R. A. Torreao, Phys. Rev. C **45** (1992) 2640.

[44] S. Bhattacharya, T. K. Das, K. P. Kanta and A. K. Ghosh, Phys. Rev. C **50** (1994) 2228.

[45] M. A. Khan, S. K. Dutta, T. K. Das and M. K. Pal, J. Phys. G: Nucl. Part. Phys. **24** (1998) 1519.

[46] Yu. A. Simonov, Yad. Fiz. **3** (1960) 630 [Sov. J. Nucl. Phys. **3** (1960)461]; in *Proc. Int. Symp. on the Present Status and Novel Developments in the Nuclear Many Body Problem*, Rome (1972), eds. F. Calogena and C. Ciofi Degli Atti, Editrice composition, Bologna (1973) p.527; Sov. J. Nucl. Phys. **7** (1968) 722.

[47] F. Zernike and H. C. Brinkman, Proc. Kon. Acad. Wtensch, **33** (1975) 3.

[48] M. Fabre de la Ripelle, Proc. Int. Sch. Nucl. Theo. Phys., Predeal (1969).

[49] M. Fabre de la Ripelle, Comp. Rendu Acad. Sci. B **269** (1970) 80; Comp. Rendu Acad. Sci. A **273** (1971) 1007.

[50] G. Erens, J. L. Visschers and R. Van Wageningen, Ann. Phys. **67** (1971) 461.

[51] J. L. Ballot, Z. Phys. A **302** (1981) 347; Few Body Systems Suppl. **1** (1986) 146.

[52] J. L. Ballot and M. Fabre de la Ripelle, Ann. Phys. (N. Y.) **127** (1980) 62.

[53] J. M. Richard, Phys. Rep. **212** (1992) 1.

[54] H. Leeb, H. Fiedeldey, E. G. O. Gavin, S. A. Sofianos and R. Lipperheide, Few Body Systems **12** (1992) 55.

[55] N. Barnea and A. Novoselsky, Ann. Phys. (N. Y.) **256** (1997) 192.

[56] S. Watanabe, Y. Hosoda and D. Kato, J. Phys. B **26** (1993) L495.

[57] B. R. Johnson, J. Chem. Phys. **69** (1978) 4678.

[58] A. K. Ghosh and T. K. Das, Fizika **22** (1990) 521.

[59] M. Abramoitz and I. A. Stegun, *Handbook of Math. Functions*, Dover Publ., New York (ninth printing) (year) p.774.

[60] J. Raynal and J. Revai, Nuovo Cimento **68** (1970) 612.

[61] T. K. Das, H. T. Coelho and M. Fabre de la Ripelle, Phys. Rev. C **26** (1982) 2281.

[62] Mayeur, J. Saction, P. Vilain, G. Wilquet et al., Nuovo Cimento B **43** (1966) 180.

[63] Y. Yamamoto and H. Bando, Prog. Theor. Phys. Suppl. **81** (1985) 9.

[64] Y. Yamamoto, T. Motoba, H. Himeno, K. Ikeda and S. Nagata, Prog. Theor. Phys. Suppl. **117** (1994) 361.

[65] M. V. Zhukov et al., Phys. Reports **231** no. 4 (1993) 141.

[66] V. I. Kukulin et al., Nucl. Phys. A **417** (1984) 128.

[67] Y. Yamamoto, H. Takaki and K. Ikeda, Prog. Theor. Phys. **86** (1991) 867.

ISTRAŽIVANJE EGZOTIČNIH HIPERJEZGRI ${}^{6}_{\Lambda\Lambda}$He HIPERSFERIČNOM METODOM TRI TIJELA

Pažljivo istražujemo dinamiku $\Lambda\Lambda$ ispitivanjem nekoliko $\Lambda\Lambda$ i $\Lambda\alpha$ fenomenoloških potencijala proučavajući svojstva vezanih stanja ${}^{6}_{\Lambda\Lambda}$He kao sustava tri tijela. Primijenili smo metodu hipersferičnih harmonika, koja je u biti egzaktna metoda za sustav tri tijela. Postigli smo konvergenciju energije vezanja do 0.07% za $K_{\max} = 20$. U ovim se računima nisu primijenila približenja ograničenjem dozvoljenih vrijednosti l međudjelujućeg para tijela.